# Evaluation of the Activity and Molecular Form of Bi in Cu Smelting Slags: Part I. Ternary Silicate Slags

S. C. MARSCHMAN and D. C. LYNCH

The thermodynamic behavior of bismuth in the chemical systems associated with copper processing is not well understood. This study was designed to further the understanding of the physical chemistry of bismuth in slags that have similar compositions to those found in copper extractive metallurgical processing. The silicate system investigated was the $FeO$-$Fe_2O_3$-$SiO_2$ ternary system in which bismuth was dissolved using an isopiestic experimental technique. Bismuth vapor pressures of $1 \cdot 10^{-5}$ atm and $7.5 \cdot 10^{-4}$ atm were used, and the silicates were equilibrated with this vapor at temperatures of 1458 K and 1523 K. In these experiments, the slag composition was varied such that $P_{O_2}$ ranged from $10^{-12}$ to $10^{-8}$ atm. Bismuth was found to enter the silicate slag in both neutral and oxidic molecular forms. The oxidic form identified was that of BiO. The data suggest that the activity coefficient of neutral bismuth, $\gamma_{Bi}$, is dependent on the solubility of that species in slag, even at the low concentrations observed in this study. It has been hypothesized, based on the large diameter of neutral Bi, that only a limited number of sites are available to accommodate neutral Bi, and that as the limit is approached $\gamma_{Bi}$ increases significantly. That hypothesis is shown to be consistent with the experimental results obtained in the present work as well as the results obtained by other investigators.

## I. INTRODUCTION

ENVIRONMENTAL contamination by minor elements associated with copper-bearing ores and concentration of those elements in blister copper are problems of increasing severity as ore quality declines. Antimony, arsenic, bismuth, selenium, and tellurium enter smelting processes in the form of sulfides, oxides, intermetallics, or as complex refractory compounds. Those elements are either volatilized, representing an air quality problem, dissolved in the discard slag, or are retained in the blister copper and thus must be removed during electrolytic refining. Selenium and tellurium are not soluble in electrolytes used in copper electrochemical refining cells, eventually being removed in the cell bottom slime. Antimony, arsenic, and bismuth are not so readily eliminated. These elements dissolve in the electrolyte as they are less noble than copper. This results in electrolyte poisoning unless careful monitoring and chemical control are exercised. These elements also will contaminate cathode copper, reducing the metal purity. Contamination of cathode copper occurs by occlusion of impure electrolyte as copper is plated out of solution at the cathodes.

The presence of trace quantities of minor elements in copper significantly reduces its ductility, electrical conductivity, and lowers its thermal conductivity. Embrittlement of copper also occurs due to impurity-phase precipitates at the copper grain boundary interfaces. These issues point out the need for an understanding of the behavior of minor elements during smelting if their concentration in blister copper is to be minimized. In this study the behavior of bismuth in silica-saturated slags was examined.

S. C. MARSCHMAN is Senior Research Engineer with Battelle Pacific Northwest Laboratories, Richland, WA 99352. D. C. LYNCH is Professor in the Department of Materials Science and Engineering at the University of Arizona, Tucson, AZ 85721.

Manuscript submitted October 21, 1987.

## II. REVIEW OF THE LITERATURE

The interaction of bismuth with slags, mattes, white metal, and blister copper has been examined by several investigators. In lieu of restricting the review to only Bi-slag interactions and for the sake of brevity, the results of those earlier investigations are summarized in Table I. Further review of those results is presented, as needed, in the discussion.

## III. EXPERIMENTAL

### A. *Isopiestic Experimental Technique*

An isopiestic technique was used to evaluate the solubility of bismuth in slag. This technique eliminates the loss of bismuth through volatilization and it allows the experimentalist to set the activity of bismuth in the system. Furthermore, as other condensed phases are not present, the isopiestic technique has the advantage of eliminating analytical errors associated with entrapment of particles of one phase in another.

During an experiment a 0.5 g slag specimen was saturated with Bi vapor at 1458 K and 1523 K using the assembly shown in Figure 1. The assembly consisted of a series of tubes and crucibles positioned such that when the assembly was inserted into the two-zone furnace, also illustrated in Figure 1, the slag became equilibrated with Bi vapor. The vapor pressure of Bi (and thus the activity of Bi) was established in each experiment by using a liquid Bi vapor source positioned at the minimum temperature between the two high-temperature zones shown in Figure 1. The liquid Bi vapor source was produced from liquified Bi shot contained in a silica crucible placed in the end of a sealed 9 mm Vycor tube.

Slag admixtures were prepared from powders of Fe, $Fe_2O_3$, and $SiO_2$. The source and purity of the chemicals used in the investigation are presented in Table II. The composition of the slags was chosen to correspond to particular oxygen potentials along the silica saturated region of the

**Table I. Review of Previous Investigations Involving Bi in Cu, Slag, and Mattes**

| Investigators | System | Results |
|---|---|---|
| Nagamori, Mackey, and Tarassoff[1] | slag-Cu | Distribution of Bi between slag and molten Cu independent of $P_{O_2}$, $l_{Bi}^{c/s} \approx 34$ at 1473 and 1573 K.* |
| See and Rankin[2] | slag-Cu | Distribution of Bi between slag and molten Cu independent of $P_{O_2}$, $l_{Bi}^{c/s} \approx 184$ at 1573 K. |
| Johnson, Sanker, Oden, and See[3] | slag-matte | Precipitated Bi-rich phase in matte at Bi content in slag between 50 and 150 ppm. |
| Goto, Ogawa, and Jimbo[4] | slag-Cu | Distribution of Bi between slag and molten Cu dependent on $P_{O_2}$, also reported existence of neutral Bi. |
| Jimbo, Goto, and Ogawa[5] | slag-Cu | Distribution of Bi between slag and molten Cu dependent on $P_{O_2}$, no neutral Bi found in slag. |
| Roine[6] | slag-matte | Distribution of Bi between slag and matte dependent on $P_{O_2}$ and $P_{S_2}$. $L_{Bi}^{s/m} = 0.436 \cdot \log(P_{O_2}) - 0.145 \log(P_{S_2}) - 0.0021$ (wt pct Cu) + 1.361.* |
| Roine and Jalkanen[7] | matte | Determined $\gamma_{Bi}^{\circ}$ in matte. $\gamma_{Bi}^{\circ}$ varied from 3.4 to 75, when sulfur-to-metal ratio of matte changed from sulfur rich to sulfur deficient. |
| Nagamori, Mackey, and Tarassoff[1] | white metal-Cu | Distribution of Bi between molten Cu and white metal varies according to the following equation: $L_{Bi}^{c/m} = 7.3 - 0.014(T - 1473)$. FeS additions decrease $L_{Bi}^{c/m}$.* |
| Asano and Wada[8] | white metal-Cu | Distribution of Bi between molten Cu and white metal reported as 8.1 at 1473 K. |
| Arac and Geiger[9] | white metal-Cu, matte-Cu, and Cu | Additions of up to 6 wt pct FeS to white metal greatly increase the activity coefficient of Bi in matte. Reported values of $\gamma_{Bi}^{\circ}$ in Cu-Bi alloy as 2.17 and 2.27 at 1473 and 1523 K, respectively.** |
| Azakami and Yazawa[10] | Cu | Experimentally determined values of $\gamma_{Bi}^{\circ}$ for Cu-Bi alloy of 4.1 at 1273 K, 3.2 at 1373 K, and 2.7 at 1473 K. |
| Sibanda and Baker[11] | Cu | Found a single value for $\gamma_{Bi}^{\circ}$ of 2.5 at 1373 K for a Cu-Bi alloy. |
| Bode, Gerlach, and Pawlek[12] (as corrected by Nagamori, Mackey, and Tarassoff[1]) | Cu | Corrected values of $\gamma_{Bi}^{\circ}$ for Cu-Bi alloy are 3.0 at 1373 K, 2.4 at 1473 K, 2.2 at 1523 K, and 2.0 at 1573 K. |
| Sigworth and Elliott[13] | Cu | Estimated value of $\gamma_{Bi}^{\circ}$ for Cu-Bi alloy of 1.25 at 1573 K. |
| Predell and Emam[14] | Cu | Reported value of $\gamma_{Bi}^{\circ}$ for Cu-Bi alloy of 2.2 at 1373 K. |
| Hildebrand and Lau[15] | slag | Examined vapors evolved from fused slag using a mass spectrometer. Bi evolved from the slag as Bi and $Bi_2$. |
| Taskinen[17] | soda-Cu | Distribution of Bi between soda and molten Cu is not markedly altered by oxygen content of the metal phase. |
| Taskinen and Niemela[18] | Cu | Experimentally determined values of $\gamma_{Bi}^{\circ}$ of 3.7, 4.5, and 5.2 at 1373, 1273, and 1173 K, respectively. |

*$l_{Bi}^{c/s} = X_{Bi}$ in Cu/$X_{Bi}$ in slag.
$L_{Bi}^{c/m}$ = wt pct Bi in Cu/wt pct Bi in matte.
$L_{Bi}^{s/m}$ = wt pct Bi in slag/wt pct Bi in matte.
**There appears to be a discrepancy in the saturation pressure used in evaluating results of this study.[9,16]

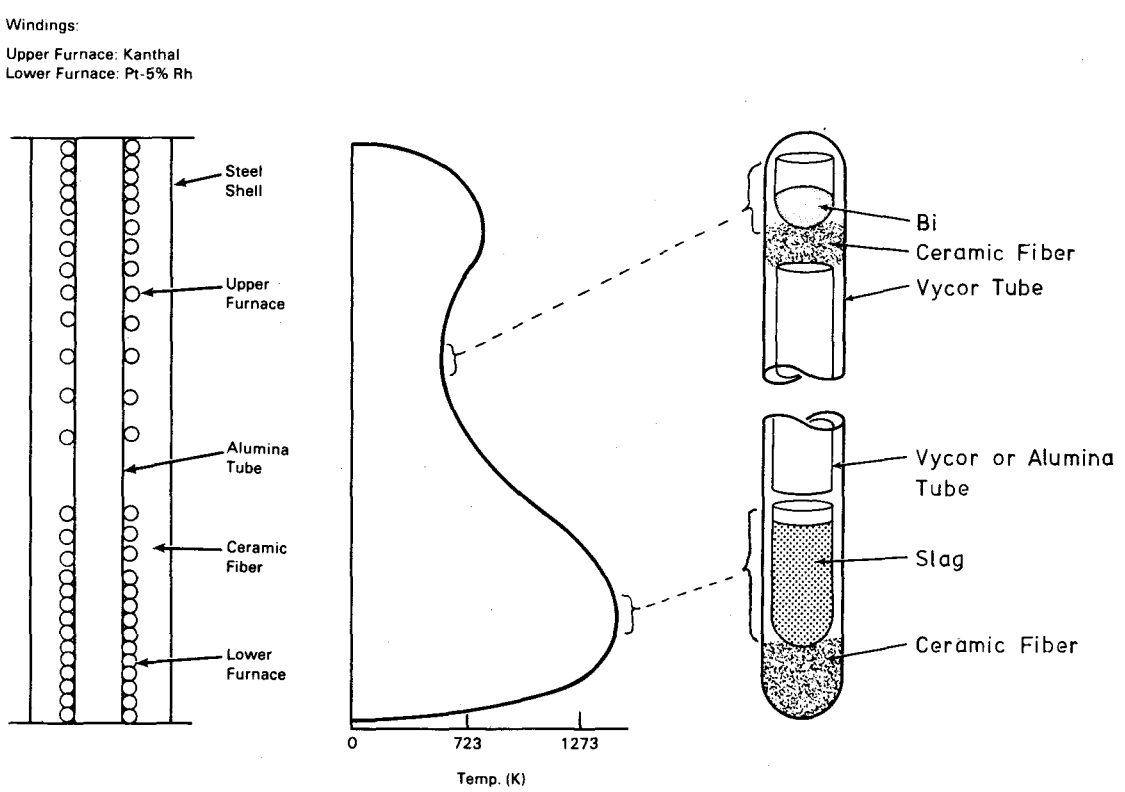


Fig. 1 — Schematic of furnace, temperature profile, and isopiestic assembly.

$FeO$-$Fe_2O_3$-$SiO_2$ phase diagram. The slag admixture was placed in a silica crucible and inserted into the other end of the 9 mm Vycor tube. The Bi- and slag-containing crucibles were separated by a vapor-porous ceramic plug, a length of 6 mm Vycor tube, and a length of 6 mm alumina tube. The distance separating the Bi- and slag-containing crucibles was determined by the temperature profile of the two-zone furnace. The temperature profile of the furnace changed slightly between the two slag temperatures used in this study, and also when the temperature was varied to change the Bi activity.

The tube assembly was evacuated to $3 \cdot 10^{-7}$ atm and heated to approximately 473 K to remove adsorbed gases from the tube walls. The assembly was then backfilled with $O_2$ (to aid in removal of $N_2$) prior to final evacuation. The assembly was then sealed under vacuum using an oxygen-acetylene flame. The presence of residual $O_2$ in the evacuated assembly did not alter the chemical system, but minimized any potential problems with thermal diffusion due to the presence of $N_2$.

**Table II. Purity of Materials Used**

| Element or Compound | Supplier | Purity | Impurities |
|---|---|---|---|
| Fe, powder (−200 mesh) | Johnson, Matthey Chemicals, Ltd. | 99.999 | Cu 5 ppm<br>Mn 3 ppm<br>Si 1 ppm<br>Ca <1 ppm<br>Mg <1 ppm |
| $SiO_2$, powder (−325 mesh) | Ventron-Alfa Division | 99.9 | — |
| $Fe_2O_3$, powder | Ventron-Alfa Division | 99.9 | 0.02 pct Fe<br>0.02 pct Mn<br>0.005 pct Zn<br>0.005 pct Cu |
| Bi, lumps | Cerac, Inc. | 99.999 | — |

The assembly was then placed in the two-zone furnace where two control circuits were used to provide a means of separately controlling the temperature of the molten Bi and slag. The slag temperature varied less than ±1 K during an experiment, while the temperature of the liquid Bi varied by no more than ±4 K. The slag was allowed to equilibrate with the vapor phase for a period of 24 or 30 hours. Lynch and Schwartze[19] found that 15 hours were adequate to saturate slag with As using the same procedure employed in the present work. Experiments with Bi revealed no difference in the concentration of Bi in slag for experiments run for 24 and 30 hours. Scanning electron microscopy (SEM) and energy dispersive X-ray analysis revealed that a homogeneous slag was formed from the admixture in 8 hours after insertion of the assembly into the furnace.

Upon completion of an experiment the assembly was quickly removed from the furnace and water quenched. Precipitation of bismuth from the cooling vapor phase was not a problem because of the relatively large thermal mass of the crucible and slag (as compared to the other components in the assembly). Bi vapor would readily condense on the cooled inner surface of the outer tube, while the heat retained by the crucible and slag prevented condensation on those surfaces. Although there was no indication of Bi precipitation on the slag specimens, a second precaution was taken to ensure that each specimen was free of condensate. After quenching, each specimen was recovered and immersed

in a HCl-$HNO_3$ solution for approximately 20 seconds to dissolve surface material. The slag specimen was then rinsed with deionized water and methyl alcohol, and allowed to dry.

### B. *Slag Digestion and Analysis for Bi*

All of the slag specimens including the crucible were ground to −100 mesh under a $N_2$ atmosphere using an agate mortar and pestle. The slag and crucible were separated using a gravimetric technique that employed 1, 1, 2, 2-tetrabromoethane as the separation medium. The 1, 1, 2, 2-tetrabromoethane has a density of 2.97 g/cm$^2$ which falls between the densities of silica and slag. The powdered slag and crucible were added to the inert fluid in a separating funnel and stirred occasionally. The separation period was 24 hours, after which the slag slurry was drained into a filter funnel and rinsed with 1-2-dichloroethane to remove any traces of 1, 1, 2, 2-tetrabromoethane. The slag then was dried at 363 K to remove any retained solvent.

Personnel at the United States Bureau of Mines[20] developed a low-cost, rapid method for digesting mineral specimens, glasses, and slags. This technique, used in the present investigation, involves digesting the specimen in an acid solution containing equal volumes of 6M HCl, 6M $HNO_3$, and 48 pct HF contained in a polycarbonate bottle at 2 atm pressure. After digesting the specimens the HF acid was neutralized with 100 ml of 1.5 wt pct boric acid solution. All of the samples were diluted to 250 ml in acid-rinsed polyethylene bottles.

The digested slags were analyzed for Bi using an Instrumentation Laboratory (IL) Model 551 atomic absorption (AA) spectrophotometer coupled to an IL655 controlled temperature furnace atomizer and Fastec™ autosampler. The AA unit was set up according to the operating procedures recommended for analysis of Bi in ultrapure water. The operating wavelength used to determine Bi was 223.1 nm, with a lamp current of 8 ma. A 0.5 nm bandpass filter was used along with deuterium background correction. The deuterium correction was deemed necessary due to the low levels of Bi contained in the slags. Testing revealed that AA standards did not require matrix matching to give accurate results. Entire groups of experiments were analyzed at a single time to reduce variation in the results. The standard deviation associated with the analytical technique was found to be 1.4 ppb for a 20 ppb solution, a concentration typical of that employed in the analysis. The standard deviation associated with the concentration presented on a fractional basis for the overall experimental procedure, *i.e.*, saturation, slag recovery, digestion, and chemical analysis, was found to be 0.36.

## IV. RESULTS

Experimental results obtained from silica-saturated iron silicate slags are presented in Table III. The quantity of Bi in each slag is reported as the mole fraction, and the slag compositions are identified by the oxygen partial pressure associated with each slag. The partial pressure of Bi in the system is also listed, and, coupled with additional thermodynamic data (presented later), can be used to determine the activity of Bi in the experimental system.

**Table III. Experimental Results for Iron-Silicate Slags**

| Slag Temp. (K) | Bi($l$) Temp. (K) | $P_{Bi}$ (atm) | $P_{O_2}$ log (atm) | $N_{Bi}$ ($\cdot 10^6$) |
|---|---|---|---|---|
| 1523 | 942 | $1 \cdot 10^{-5}$ | −12 | 2.5 |
| | | | −11 | 1.5 |
| | | | −10 | 1.6 |
| | | | − 9 | 16. |
| | | | − 8 | 22. |
| | | | − 8 | 16. |
| 1523 | 1131 | $7.5 \cdot 10^{-4}$ | −12 | 2.1 |
| | | | −12 | 4.4 |
| | | | −12 | 2.1 |
| | | | −11 | 8.3 |
| | | | −10 | 24. |
| | | | − 9 | 72. |
| | | | − 9 | 89. |
| | | | − 8 | 470. |
| | | | − 8 | 260. |
| 1458 | 942 | $1 \cdot 10^{-5}$ | −12 | 5.9 |
| | | | −12 | 11. |
| | | | −11 | 8.4 |
| | | | −10 | 3.7 |
| | | | −10 | 6.4 |
| | | | − 9 | 13. |
| | | | − 8 | 15. |
| | | | − 8 | 13. |
| | | | − 8 | 20. |
| 1458 | 1131 | $7.5 \cdot 10^{-4}$ | −12 | 3.8 |
| | | | −12 | 7.2 |
| | | | −12 | 1.0 |
| | | | −11 | 24. |
| | | | −11 | 8.1 |
| | | | −10 | 16. |
| | | | −10 | 22. |
| | | | − 9 | 160. |
| | | | − 9 | 200. |
| | | | − 8 | 90. |
| | | | − 8 | 360. |

## V. DISCUSSION

The isopiestic technique, like all techniques, has both advantages and disadvantages. The advantages of this type of experimental system were identified in a previous section. Disadvantages of the isopiestic system include long equilibration times, thermal and Knudsen diffusion problems, and precipitation of unwanted phases.

The equilibration time of these experiments was reduced to 24 hours by using relatively small (500 mg) slag samples. The influence of thermal diffusion was minimized by ensuring that the total vapor pressure of bismuth was several orders of magnitude greater than any other vapor species. The influence of Knudsen diffusion was minimized by ensuring that the mean free path of the vapor species was much smaller than the diameter of the vapor pathway in the assembly. Thermodynamic calculations and visual observations were used to verify that only elemental vapor species were present within the experimental system. Analysis of these potential disadvantages begins with an examination of the potential for formation of unwanted vapor species.

A. *Analysis of the Bi-O Vapor System*

The species found in the Bi-O vapor system are numerous. Researchers have reported finding the species BiO, $Bi_2O$, $Bi_2O_2$, $Bi_2O_3$, $Bi_3O_3$, $Bi_3O_4$, $Bi_4O_4$, $Bi_4O_6$, and $Bi_5O_7$.[21–25] Thus, the Bi-O vapor system is complicated by the large number of bismuth oxides and the inconsistencies among the few studies conducted to evaluate this system.

The authors consider the work by Sidorov *et al.*[21] to be the most authoritative study to date. Using mass spectrometry to examine vapor evolved from pure $Bi_2O_3$, they reported the species Bi, $O_2$, BiO, $Bi_2O$, $Bi_2O_2$, $Bi_2O_3$, $Bi_3O_4$, and $Bi_4O_6$ as parent molecules. The thermodynamic data from their study have been reformed into equations that yield standard Gibbs energy extrapolated to 1600 K. The results are presented in Table IV.

The data in Table IV have been used to estimate the extent of Bi oxide formation for a worst case scenario. The results of that analysis are presented in Figures 2 and 3. The data in those figures were obtained by assuming $P_{O_2}$ to be $10^{-8}$ atm and $P_{Bi}$ to have values of $10^{-5}$ and $10^{-2}$ atm. At the lower values for $P_{Bi}$, the elemental vapor pressure is estimated to be at least 3 orders of magnitude greater than the vapor pressure of the most predominant oxide, BiO. At the higher value of $P_{Bi}$ a similar situation exists except the calculations suggest that $Bi_2O$ is the predominant oxide. It is also evident from the data in Figures 2 and 3 that at lower temperatures the oxide vapors become predominant, and that precipitation of $Bi_4O_6$ vapor as liquid $Bi_2O_3$ on the inner wall of the cooler portion of an experiment tube should occur.

The latter suggestion is inconsistent with the experimental results, where only grey metallic Bi precipitate was found after quenching. Any significant presence of $Bi_2O_3$ would have been detected visually, as the stable high-temperature rhombohedral form of the oxide has a distinctive yellow color. No such precipitate was observed in any of the experiments. It is expected that further refinement of the thermodynamic data will reconcile those differences.

The thermodynamic data for the four forms of elemental Bi, for which there is agreement among investigators, was used to evaluate the molecular components of elemental Bi vapor.[26–30] The results of that analysis are presented in Figure 4 where partial pressures of Bi, $Bi_2$, $Bi_3$, and $Bi_4$ are plotted as a function of the source temperature (temperature of liquid Bi during an experiment). The analysis reveals that monatomic Bi is the predominant form and that its vapor pressure does not change appreciably with variations in the slag temperature.

B. *Thermal Separation of Gaseous Species*

It is well documented that whenever a temperature gradient exists, there will be a partial separation of the gas components. This is known as the Soret effect and is characterized by movement of heavier molecules toward the low temperature, while lighter molecules move toward the higher temperature.

Incorrect estimates of the vapor pressure of a species in an isopiestic experiment can be made if the Soret effect plays an important role in the movement of gas molecules within the experimental system. Thermal separation among Bi, $Bi_2$, $Bi_3$, and $Bi_4$ is countered by chemical reactions between the species in the present work. However, since both processes, separation and chemical reactions, are rate processes and it is not known which of these processes is rate controlling, it is essential that the extent of the Soret effect be evaluated.

The analysis presented earlier suggests that the vapor phase within an isopiestic experiment tube consists primarily of Bi, $Bi_2$, $Bi_3$, $Bi_4$, and $O_2$. The partial pressure of oxygen is associated with the slag composition and ranged from $10^{-12}$ to $10^{-8}$ atm. The partial pressure of Bi and $Bi_2$ are three orders of magnitude or more greater than the partial pressure of $O_2$ except at the highest value of the ferrous/ferric ion ratio. The vapor consists essentially of Bi and $Bi_2$ and because the concentrations of the other species are so much smaller, only the former need be considered in analysis of the Soret effect.

Due to the Soret effect, $Bi_2$ will tend to diffuse toward the lower temperature where liquid bismuth is vaporized, and Bi will diffuse toward the higher temperature where the slag

**Table IV. Standard Gibbs Energy Equations for Bismuth Vapor Species (545 K to 1600 K)**

| | $\Delta G^\circ = A + BT + CT \ln T + DT^2 + E/T$ (J/mol) | | | | |
|---|---|---|---|---|---|
| Reaction | *A* | *B* | *C* | *D* | *E* |
| Bi(l) = Bi(g)* | 190523 | − 100.3 | | | |
| $Bi_2(g) = 2Bi(g)$ | 197360 | − 105.9 | | | |
| $Bi_3(g) = 3Bi(g)$ | 319671 | − 231.1 | | | |
| $Bi_4(g) = 4Bi(g)$ | 583571 | − 348.1 | | | |
| $Bi(g) + \frac{1}{2}O_2 = BiO(g)$ | − 97000 | − 84.0 | 2.6 | −0.22 | $5.85 \cdot 10^6$ |
| $2Bi(g) + \frac{1}{2}O_2 = Bi_2O(g)$ (linear) | − 706200 | 2533 | 310 | 0.06 | $7.4 \cdot 10^7$ |
| $2Bi(g) + \frac{1}{2}O_2 = Bi_2O(g)$ (angular) | $2.9 \cdot 10^6$ | − 24175 | 3290 | −1.1 | $-5.0 \cdot 10^8$ |
| $2Bi(g) + O_2 = Bi_2O_2(g)$ | $2.6 \cdot 10^6$ | 65230 | 3190 | −1.1 | $-4.8 \cdot 10^8$ |
| $4Bi(g) + 3O_2 = Bi_4O_6(g)$ | $-1.24 \cdot 10^6$ | − 4860 | 818 | −0.46 | − 27350 |
| $3Bi(g) + 2O_2 = Bi_3O_4(g)$ | $4.5 \cdot 10^6$ | − 43560 | 6010 | −2.21 | $-8.2 \cdot 10^8$ |
| $2Bi(g) + \frac{3}{2}O_2 = Bi_2O_3(g)$ | $8.8 \cdot 10^6$ | − 70770 | 9590 | −3.16 | $-1.5 \cdot 10^9$ |

*The standard state of bismuth chosen for these calculations was the pure liquid. Thus, the temperature range of these equations is limited at the lower end to 545 K. Pankratz provided the enthalpy of fusion for bismuth, and equations for the heat capacities of solid and liquid bismuth.[26] These are reproduced here:

Bi(s), 298.15 to 545 K: $C_p = 13.903 + 2.680 \cdot 10^{-2}T + 3.226\ 10^5 T^{-2}$ (J/mol K)

Bi(l), 545 to 1600 K: $C_p = 24.490 + 6.653 \cdot 10^{-7}T + 1.580 \cdot 10^6 T^{-2}$ (J/mol K)

$\Delta H_f^\circ = 11.3$ kJ

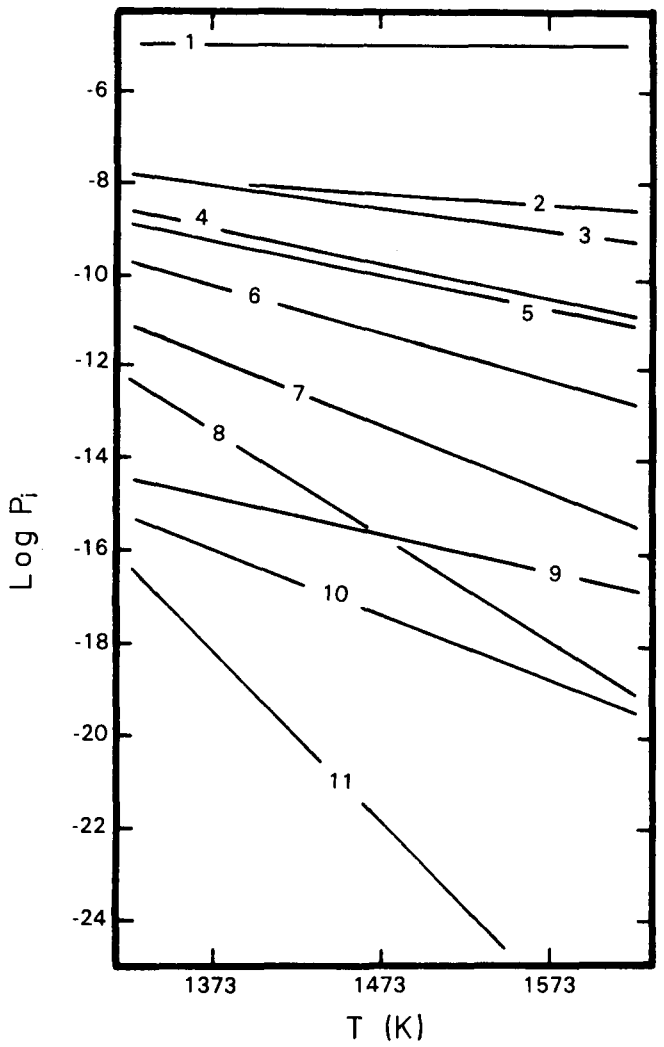


Fig. 2—The partial pressure of molecular and oxide species of bismuth at $P_{Bi} = 1.0 \cdot 10^{-5}$ atm and $P_{O_2} = 1.0 \times 10^{-8}$ atm. The numbers correspond to the following species: (1) Bi; (2) BiO; (3) $Bi_2$; (4) $Bi_2O$ (angular); (5) $Bi_2O$ (linear); (6) $Bi_2O_2$; (7) $Bi_2O_3$; (8) $Bi_3O_4$; (9) $Bi_3$; (10) $Bi_4$; (11) $Bi_4O_6$.

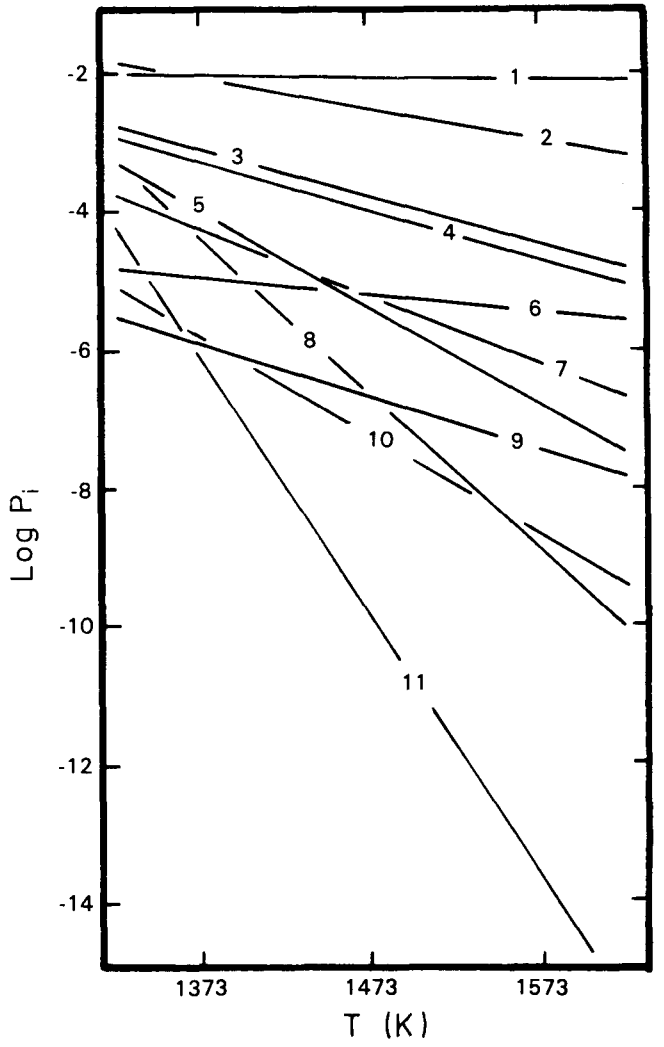


Fig. 3—The partial pressure of molecular and oxide species of bismuth at $P_{Bi} = 1.0 \cdot 10^{-2}$ atm, and $P_{O_2} = 1.0 \cdot 10^{-8}$ atm. The numbers correspond to the following species: (1) Bi; (2) $Bi_2$; (3) $Bi_2O$ (angular); (4) $Bi_2O$ (linear); (5) $Bi_4$; (6) BiO; (7) $Bi_2O_2$; (8) $Bi_3O_4$; (9) $Bi_3$; (10) $Bi_2O_3$; (11) $Bi_4O_6$.

melt is located. The importance of this phenomenon can be evaluated by examining the mass flux and its dependence on the temperature gradient. The mass flux, $j_i$, for a multicomponent system can be represented by the following equation:

$$j_i = j_i^X + j_i^P + j_i^g + j_i^T \qquad [1]$$

The superscripts $X$, $P$, $g$, and $T$ represent the concentration diffusion, pressure diffusion, forced diffusion, and thermal diffusion, respectively. There can be no mass flux contribution due to pressure in an isopiestic system since the pressure within the tube is constant. Additionally, since the only external force acting on the system is gravity, the forces on each vapor component were equal, and therefore the term $j_i^g$ disappears. The remaining terms, $j_i^X$ and $j_i^T$, can be used to derive Eq. [2], as

$$X_{A2} - X_{A1} = k_T \ln \frac{T_2}{T_1} \qquad [2]$$

where $X_{A2}$ and $X_{A1}$ represent the vapor phase mole fractions of $A$ at $T_2$ and $T_1$, respectively. Equation [2] shows that the variation in composition, $X_{A2} - X_{A1}$, due to a thermal gradient is dependent on variation in temperature and the thermal diffusion ratio, $k_T$. The latter is dependent on the mass and size of the gas species, the nature of the intermolecular forces between molecules, and the concentration of the species. The nature of the dependency is also described in Appendix A.

Analysis of $k_T$ and Eq. [2] lead to the results reported in Table V. Calculated values for $k_T$ range from $-0.012$ to $-0.023$. Negative values for $k_T$ are not unusual and indicate that the heavy gaseous species move to the cooler section of the vessel. Values of the separation, $X_{A2} - X_{A1}$, for Bi (and $Bi_2$) range from 0.001 to a maximum of 0.01. Since $X_{Bi}$ approaches unity throughout the isopiestic experiment tube assembly, the influence of the Soret effect on relating the solubility of Bi in the slag to the calculated vapor pressure over the slag is expected to be small.

### C. *Knudsen Diffusion*

Knudsen diffusion can alter the concentration of vapor species over a melt from that calculated from thermody-

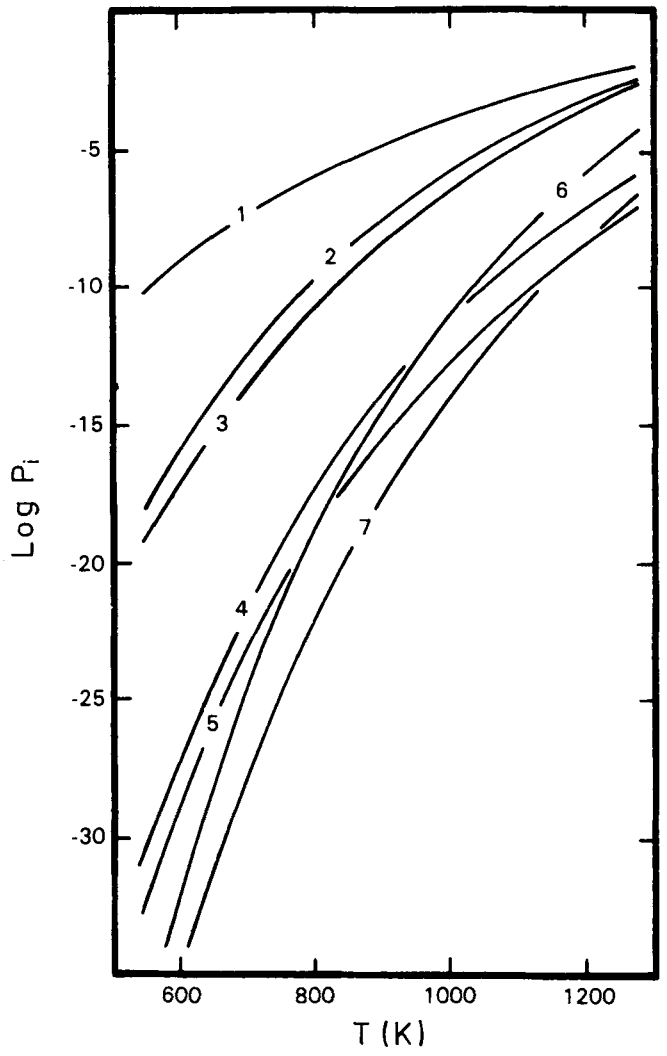


Fig. 4—Bismuth vapor at 1458 K and 1523 K when emanated from liquid bismuth at a low source temperature (X-axis). The total pressure is fixed by the saturation pressure at the source temperature. The curves are numbered as follows: (1) Bi at 1458 K and 1523 K; (2) $Bi_2$, 1458 K; (3) $Bi_2$, 1523 K; (4) $Bi_3$, 1458 K; (5) $Bi_3$, 1523 K; (6) $Bi_4$, 1458 K; (7) $Bi_4$, 1523 K.

namics in an isopiestic system where low pressures are employed and narrow tubes are involved. Knudsen diffusion is an issue only if the Bi and $Bi_2$ vapors do not readily react to establish thermodynamic equilibrium. The importance of Knudsen diffusion must be evaluated since the appropriate kinetic data are not available for the system used in this study.

The standard test for evaluating the role of Knudsen diffusion involves evaluating the ratio of molecular diffusivity to Knudsen diffusivity,[31] $D_{AB}/D_K$. Ordinary molecular diffusion predominates if the ratio is small, and the influence of Knudsen diffusion on the vapor phase equilibrium is negligible. Values for $D_{Bi-Bi_2}$ and $D_K$ listed in Table VI were calculated using standard procedures. The values of $D_{Bi-Bi_2}/D_K$ reveal that Knudsen diffusion had little or no effect on the equilibrium process.

**Table V. Values of the Thermal Diffusion Ratio and the Separation Due to Thermal Mass Diffusion**

| Slag Temp. (K) | Source Temp. (K) | Mean Temp. (K) | $k_T$ | $X_{A2} - X_{A1}$ |
|---|---|---|---|---|
| 1458 | 942 | 1162 | −0.023 | 0.010 |
| 1523 | 942 | 1186 | −0.012 | 0.0010 |
| 1458 | 1131 | 1281 | −0.018 | 0.0045 |
| 1523 | 1131 | 1308 | −0.014 | 0.0040 |

### D. *Phase Rule Considerations*

In any equilibrium study it is essential to identify the state of the system. This is usually accomplished by fixing external variables such as temperature, total pressure, and the partial pressures of reactive vapor species. Static systems, such as the isopiestic system used in this study, pose additional problems since only the temperature can be fixed externally.

The number of variables that must be set to fix the state of the system can be calculated from the Gibbs phase rule:

$$F = C - N - P + 2 - R \qquad [3]$$

where $F$ is the degrees of freedom, $C$ is the number of components, $N$ is the number of independent chemical reactions which occur between the components, $P$ is the total number of phases, and $R$ represents any stoichiometric restrictions. An iron silicate slag is composed of $Fe_2O_3$, FeO, and $SiO_2$. At equilibrium, the slag will establish a gas phase consisting of $O_2$. This system consists of 4 components, and if the slag is contained in a silica crucible, $P$ is 3. One independent chemical reaction can be written between FeO, $Fe_2O_3$, and $O_2$. Accordingly, for an iron silicate slag contained in a silica crucible, $F$ is 2. The state of the slag can be fixed by setting the temperature and the ferrous/ferric ion ratio.

Normally, wet chemical methods are used to find the ferrous/ferric ion ratio of a slag. These methods are well documented in the literature and generally require a sample of 1 to 2 grams for accurate results.[32] In this study only 500 mg slag samples were used. Upon completion of an experiment, a maximum of 80 pct of the slag was recovered. Bi analysis required 200 to 250 mg of slag, leaving between 50 and 150 mg of slag for iron analysis. This quantity was too small for accurate wet chemical determination of the ferrous/ferric ion ratio. Subsequently, a more suitable method was developed based on the procedure proposed by

**Table VI. Ordinary Diffusion Coefficients, Knudsen Diffusion Coefficients, and Their Ratio for the Bi-$Bi_2$ Vapor System**

| Mean Temp. (K) | $P$ (atm) | $D_{Bi-Bi_2}$ ($cm^2$/sec) | $D_{k,Bi}$ ($cm^2$/sec) | $D_{k,Bi_2}$ ($cm^2$/sec) | $\frac{D_{Bi-Bi_2}}{D_{k,Bi}}$ | $\frac{D_{Bi-Bi_2}}{D_{k,Bi_2}}$ |
|---|---|---|---|---|---|---|
| 1162 | $1.0 \cdot 10^{-5}$ | 0.020 | 4310 | 3047 | $4.6 \cdot 10^{-6}$ | $6.6 \cdot 10^{-6}$ |
| 1186 | $1.0 \cdot 10^{-5}$ | 0.024 | 4622 | 3268 | $5.2 \cdot 10^{-6}$ | $7.3 \cdot 10^{-6}$ |
| 1281 | $7.5 \cdot 10^{-4}$ | 0.00035 | 4803 | 3396 | $7.3 \cdot 10^{-8}$ | $1.0 \cdot 10^{-7}$ |
| 1308 | $7.5 \cdot 10^{-4}$ | 0.0004 | 4853 | 3432 | $8.2 \cdot 10^{-8}$ | $1.2 \cdot 10^{-7}$ |

Harvey, Smart, and Amis.[33] The procedure is discussed in Appendix B.

The hypothesis regarding the preparation of slag from powders of Fe, $Fe_2O_3$, and $SiO_2$ and the ferrous/ferric ion ratio was checked. Iron powder was used instead of wustite because the latter is not stoichiometric. The Fe and $Fe_2O_3$ were mixed in the appropriate amounts to ensure the desired ferrous/ferric ion ratio. The results of this test are presented in Table VII and reveal that the desired slag compositions could be achieved with the isopiestic technique.

The addition of Bi to the system offers an additional degree of freedom, in that $C$ is now 5. With the isopiestic technique the partial pressure of Bi above the slag is known, the slag is contained in a silica crucible, the temperature is set, and the ferrous/ferric ratio of the slag is known.* Thus, the system is fixed. Accordingly, externally controlled factors can be used to specify the state of a silica-saturated iron silicate slag in an isopiestic experiment.

*Dissolution of bismuth in the slag as the oxide alters the ferrous/ferric ion ratio. The influence of the dissolution of bismuth on this ratio was estimated from mass balance considerations and found to be insignificant for the solubilities reported in this study.

### E. *Dissolution Models*

Nagamori *et al.* proposed that minor elements dissolve in slag in either an elemental form, as oxides, or metallides.[1,34] They also proposed that combinations of these forms can exist.

*Metallides.* A decrease in $P_{O_2}$ at silica saturation moves the slag composition toward iron saturation, which must be accompanied by an increase in the activity of iron, $a_{Fe}$. Nagamori and Mackey postulated that the increase in $a_{Fe}$ can result in the formation of iron metallides, and that such behavior would be characterized by an increase in solubility of the minor element in slag with decreasing values[34] of $P_{O_2}$. They found that the dissolution of Se in slag exhibited that behavior. Fang and Lynch confirmed those results and showed that bonding in a metallide complex is similar to that of intermetallic compounds formed in the binary system.[35]

The Bi-Fe phase diagram reveals that those elements do not form any intermetallics, and that they are mutually immiscible. According to the results of Fang and Lynch, formation of Bi-Fe metallide complexes in slag is not expected to occur.

*Elemental and Oxidic Bismuth.* Elemental and oxidic dissolution of Bi in silicates can be represented by the following reactions:

$$1/x\mathrm{Bi}_x(g) = \mathrm{Bi}(slag) \qquad [4]$$

$$1/x\mathrm{Bi}_x(g) + \phi\mathrm{O}_2 = \mathrm{BiO}_{2\phi}(slag) \qquad [5]$$

The equilibrium constants of these reactions can be written in terms of activity coefficients, mole fractions, and partial pressures of the species involved in each reaction. These equations are, respectively:*

*$N$ is used to represent mole fractions in condensed phases whereas $X$ is used for the same purpose when characterizing gases.

$$\frac{N_{Bi}}{(P_{Bi_x})^{1/x}} = \frac{K_{eq[4]}}{\gamma_{Bi}} \qquad [6]$$

$$\frac{N_{BiO_{2\phi}}}{(P_{Bi_x})^{1/x}} = \frac{K_{eq[5]}(P_{O_2})^{\phi}}{\gamma_{BiO_{2\phi}}} \qquad [7]$$

Equation [6] indicates that if elemental dissolution is the only mechanism by which Bi enters slag the mole fraction of Bi is dependent only upon the partial pressure of Bi over the slag, if the activity coefficient remains constant. Equation [7] indicates that if oxidic dissolution of Bi in slag predominates, then the concentration of Bi in slag will be dependent upon both the oxygen and bismuth partial pressure in the experimental system.

The possibility exists for an overall dissolution of Bi in slag which is a combination of both elemental and oxidic dissolution processes. This process may be represented by the mass balance:

$$n^t = n^o + n^e \qquad [8]$$

where the $t$, $o$, and $e$ represent the total moles, moles due to oxidic dissolution, and the moles present due to elemental or neutral dissolution. The mole fraction of Bi in slag may be found by dividing Eq. [8] by the total moles of slag, which yields:

$$N^t = N^o + N^e \qquad [9]$$

Equation [9] can be expanded by substitution of Eqs. [6] and [7] for the terms $N^o$ and $N^e$, which yields:

$$\frac{N^t}{(P_{Bi_x})^{1/x}} = \frac{K_{eq[4]}}{\gamma_{Bi}} + \sum_{\phi=1/2,\,3/4\ldots} \frac{K_{eq[5]}(P_{O_2})^{\phi}}{\gamma_{BiO_{2\phi}}} \qquad [10]$$

The second term in Eq. [10] accounts for the possibility that more than one bismuth oxide may exist in slag. This equation provides a model for relating the solubility of Bi in slag to the partial pressure of $O_2$ in the experimental system.

### F. *Solubility in Ternary Slags*

The solubility data presented in Table III are plotted in Figures 5 through 8 as a function of the partial pressure of $O_2$ associated with each slag. The data indicate two apparent trends in the dissolution behavior of Bi in slag. Experiments performed at lower partial pressures of $O_2$ and Bi indicated the solubility of Bi in slag was essentially independent of the partial pressure of $O_2$. Experiments performed at the higher partial pressure of Bi indicated the solubility of Bi in slag was found to increase with increasing oxygen partial pressure.

Linear regression analysis performed on the data in Figures 5 and 7 yielded no regression curves. These data, particularly at the lower values of $P_{O_2}$, best fit the condition of elemental dissolution of Bi in slag. Linear regression analysis of the data contained in Figures 6 and 8 yielded the following regression equations:

**Table VII. Comparison of Predicted Ferrous/Ferric Ion Ratios to Experimentally Determined Ratios**

| Log $P_{O_2}$ (atm) | Calculated Ferrous/Ferric Ratio | Experimentally Determined Ferrous/Ferric Ratio |
|---|---|---|
| −11 | 12.7 | 11.6 |
| − 8 | 3.9 | 2.8 |
| − 8 | 3.9 | 3.0 |
| − 8 | 3.9 | 6.9 |

$$\log N_{Bi} = 0.47 \log P_{O_2} + 0.19 \quad \text{(Figure 6)} \quad [11]$$

$$\log N_{Bi} = 0.52 \log P_{O_2} + 0.64 \quad \text{(Figure 8)} \quad [12]$$

At a fixed bismuth activity, rearranging Eq. [7] yields the following proportionality:

$$\log N_{BiO_{2\phi}} \propto \phi \log P_{O_2} \quad [13]$$

The slopes of the lines in Figures 6 and 8 are indicative of oxidic dissolution of bismuth in slag. Assuming all the bismuth enters the slag as an oxide, Eq. [13] can be reformed to yield:

$$\log N_{Bi} = \phi \log P_{O_2} + \text{constant} \quad [14]$$

as $N_{Bi}$ under the stated condition equals $N_{BiO_{2\phi}}$. The regression slopes in Eqs. [11] and [12] suggest that $\phi$ has a value of 0.5 and that bismuth dissolves in slag, for the conditions noted in Figures 6 and 8, as BiO.

Utilizing 0.5 for the value of $\phi$, Eq. [10] may be rewritten as,

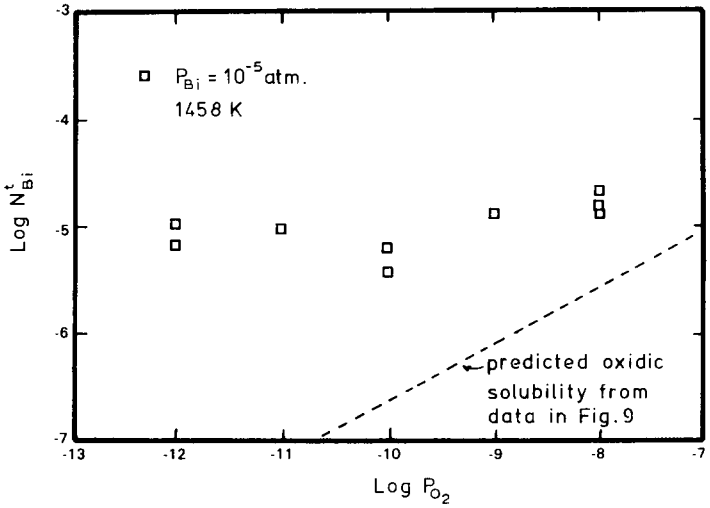


Fig. 5—Ternary slag results plotted as log $N_{Bi}$ *vs* log $P_{O_2}$ ($P_{Bi} = 1 \cdot 10^{-5}$ atm, $T = 1458$ K).

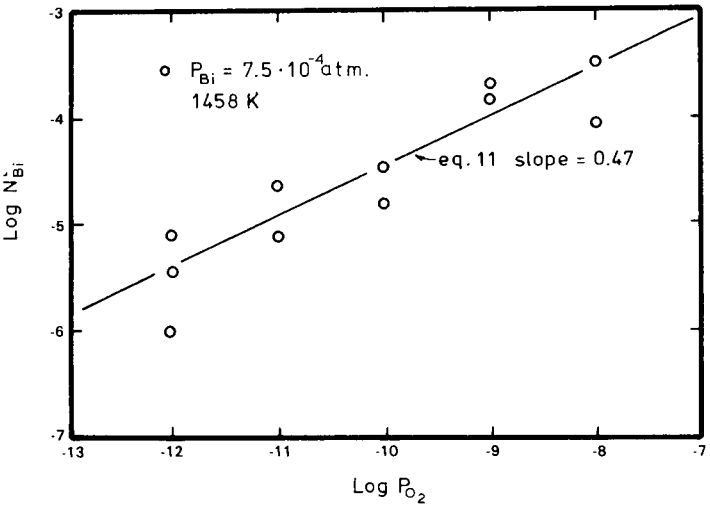


Fig. 6—Ternary slag results plotted as log $N_{Bi}$ *vs* log $P_{O_2}$ ($P_{Bi} = 7.5 \cdot 10^{-4}$ atm, $T = 1458$ K).

$$\frac{N^t}{P_{Bi}} = \frac{K_{eq[4]}}{\gamma_{Bi}} + \frac{K_{eq[5]}(P_{O_2})^{1/2}}{\gamma_{BiO}} \quad [15]$$

The data in Figures 6 and 8 were plotted as functions of $N_t/P_{Bi}$ *vs* $P_{O_2}^{1/2}$ in Figure 9. Regression analysis of these data yielded the following equations:

$$N^t/P_{Bi} = 0.026 + 3080(P_{O_2})^{1/2} \quad (1458 \text{ K}) \quad [16]$$

$$N^t/P_{Bi} = 0.003 + 4710(P_{O_2})^{1/2} \quad (1523 \text{ K}) \quad [17]$$

These equations as recommended by Goto *et al.* were coupled with thermodynamic data for Bi and BiO and used to calculate the activity coefficients for those species in slag.[4,5] The thermodynamic data for liquid Bi was obtained from Pankratz,[26] while thermodynamic data for BiO were estimated using procedures recommended by Kubaschewski and Alcock.[36] The derived thermodynamic relationships are:

$$\text{Bi(g)} + \frac{1}{2}\text{O}_2 = \text{BiO(l)}$$

$$\Delta G^\circ = -603{,}084 + 193.14 \cdot T \quad \text{J/mol} \quad [18]$$

$$\text{Bi(g)} = \text{Bi(l)}$$

$$\Delta G^\circ = -190{,}568 + 100.3 \cdot T \quad \text{J/mol} \quad [19]$$

Equilibrium constants for these reactions are listed in Table VIII. The coefficients in Eqs. [16] and [17] may be directly substituted for the appropriate terms in Eq. [15]. Knowledge of the equilibrium constants for reactions [18] and [19] leads directly to the resolution of the values of $\gamma_{Bi}$ and $\gamma_{BiO}$ in slag. These values are listed in Table IX.

The fraction of Bi in slag existing in an oxidic form or elemental form was calculated by dividing Eq. [15] and rearranging the result as follows for elemental dissolution:

$$f_{Bi}^e = \left(\frac{N^e}{N^t}\right)_{Bi} = \frac{1}{1 + \dfrac{\gamma_{Bi} K_{eq[18]}(P_{O_2})^{1/2}}{\gamma_{BiO} K_{eq[19]} P_{Bi}}} \quad [20]$$

and for oxidic dissolution:

$$f_{Bi}^o = \left(\frac{N^o}{N^t}\right)_{Bi} = \frac{1}{\dfrac{\gamma_{BiO} K_{eq[19]} P_{Bi}}{\gamma_{Bi} K_{eq[18]}(P_{O_2})^{1/2}} + 1} \quad [21]$$

These equations show that both forms of bismuth in slag depend on the partial pressures of $O_2$ and Bi, and on temperature when mixed dissolution processes occur. Either Eq. [20] or [21] can be used to plot the fraction of Bi in both elemental and oxidic forms in slag as a function of $P_{O_2}$. Such plots are shown in Figures 10 and 11 at $P_{Bi}$ equal to $7.5 \cdot 10^{-4}$ atm.

The solubility results at the lower partial pressure of bismuth show mixed results (see Figures 5 and 7). In those experiments the solubility of bismuth appears to be independent of the oxygen potential at the lower values of $P_{O_2}$. At the higher values of $P_{O_2}$, however, there is an indication of oxidic dissolution, particularly for the results obtained at 1523 K.

The anticipated solubility of BiO in slag is represented as dotted lines in Figures 5 and 7. Those lines were calculated using the values of $\gamma_{BiO}$ in Table IX and Equation [18]. It is interesting to note that there is apparent agreement in the solubility data and the predicted behavior for oxidic dissolution. The effect of oxidic dissolution in the experimental data is more pronounced at 1523 K (see Figure 7) than the

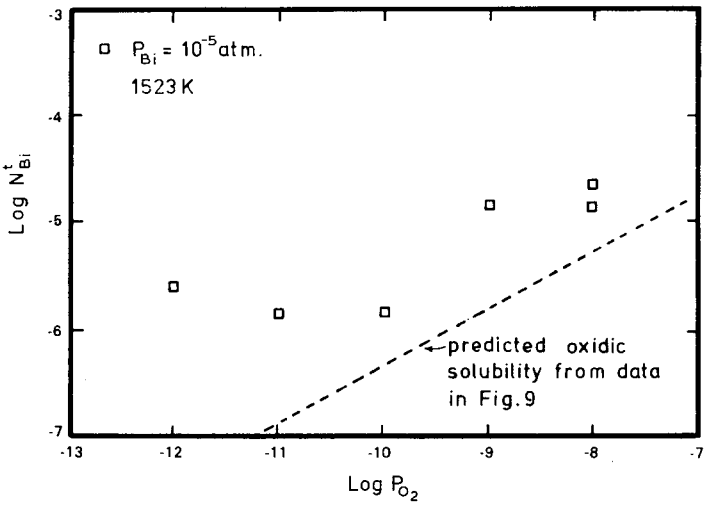


Fig. 7—Ternary slag results plotted as log $N_{Bi}$ *vs* log $P_{O_2}$ ($P_{Bi} = 1 \cdot 10^{-5}$ atm, $T = 1523$ K).

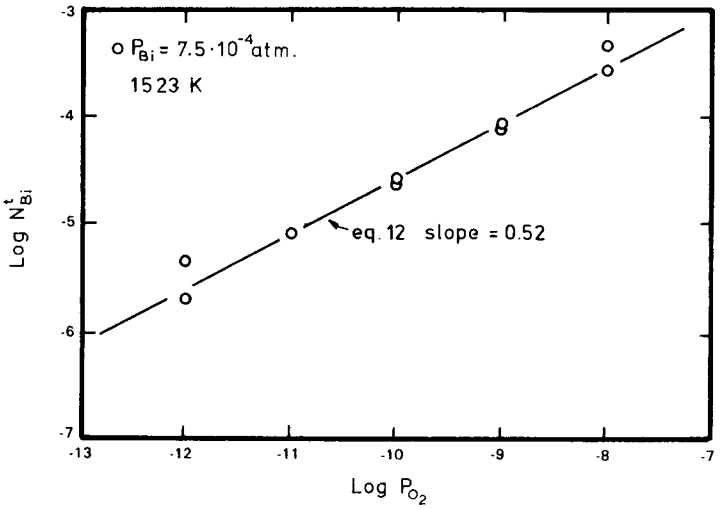


Fig. 8—Ternary slag results plotted as log $N_{Bi}$ *vs* log $P_{O_2}$ ($P_{Bi} = 7.5 \cdot 10^{-4}$ atm, $T = 1523$ K).

**Table VIII. Thermodynamic Quantities for the Formation of Bi(l) and BiO(l)**

| Reaction | Temp. (K) | $\Delta G°$ (J/mol) | $K_{eq}$ |
|---|---|---|---|
| Bi(g) = Bi(l) | 1458 | − 44,300 | 38.64 |
| | 1523 | − 37,780 | 19.76 |
| Bi(g) + $\frac{1}{2}O_2$ = BiO(l) | 1458 | −321,415 | $3.27 \cdot 10^{11}$ |
| | 1523 | −308,860 | $3.92 \cdot 10^{10}$ |

**Table IX. Experimentally Derived Values for $\gamma_{Bi}$ and $\gamma_{BiO}$ in Slag**

| $P_{Bi}$ (atm) | Temp. (K) | $\gamma^*_{Bi}$ | $\gamma^*_{BiO}$ |
|---|---|---|---|
| $7.5 \cdot 10^{-4}$ | 1458 | 1500 | $1.1 \cdot 10^8$ |
| | 1523 | 6600 | $8.3 \cdot 10^6$ |
| $1.0 \cdot 10^{-5}$ | 1458 | 55 | |
| | 1523 | 106 | |

*liquid standard state

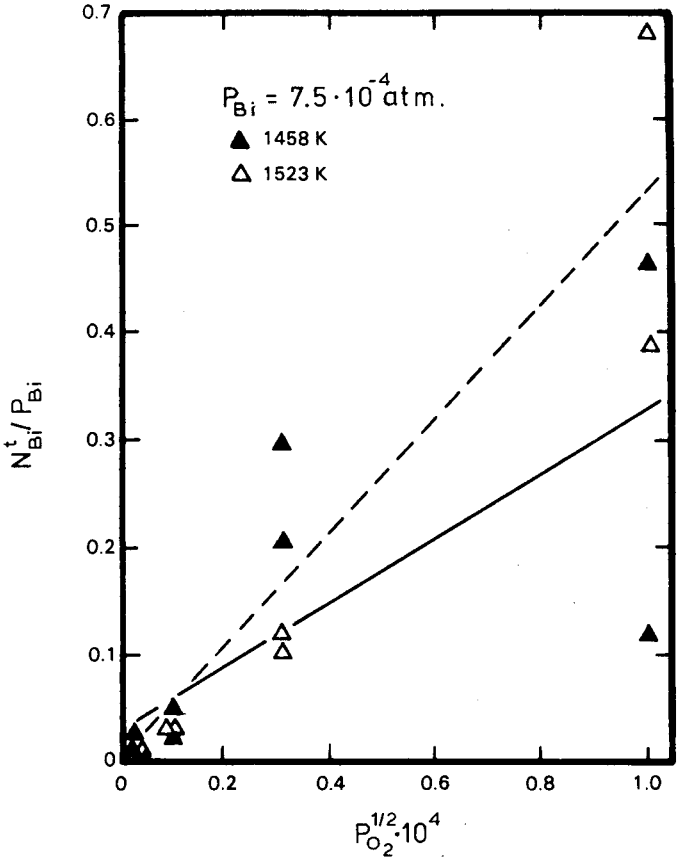


Fig. 9—Solubility of bismuth in silica-saturated slags as represented by Eq. [15] ($P_{Bi}$=$7.5 \cdot 10^{-4}$ atm).

data in Figure 5 at 1458 K. The predicted solubility yields the same results. The discrepancy in the predicted solubility of BiO and the actual data is not unexpected given the uncertainty in the regression analysis used to obtain the values of $\gamma_{BiO}$ in Table IX. That uncertainty is typical of the results obtained with Eq. [15].[4,5] In evaluating Eq. [15], the uncertainty in data collected at the higher values of $P_{O_2}$ has a disproportionate effect on the regression slope.

Values of $\gamma_{Bi}$ calculated from the solubility data in Figures 5 and 7 are also reported in Table IX. Equation [6] and, only, the solubility data obtained at values of $P_{O_2} < 10^{-10}$ atm were used in the calculations. The tabulated values of $\gamma_{Bi}$ obtained from data in Figures 5 and 7 may be

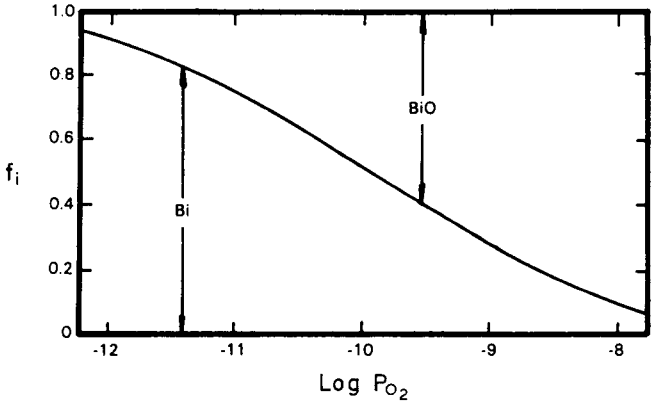


Fig. 10—Fraction of the two forms of bismuth in slag at 1458 K and $P_{Bi}$ equal to $7.5 \cdot 10^{-4}$ atm.

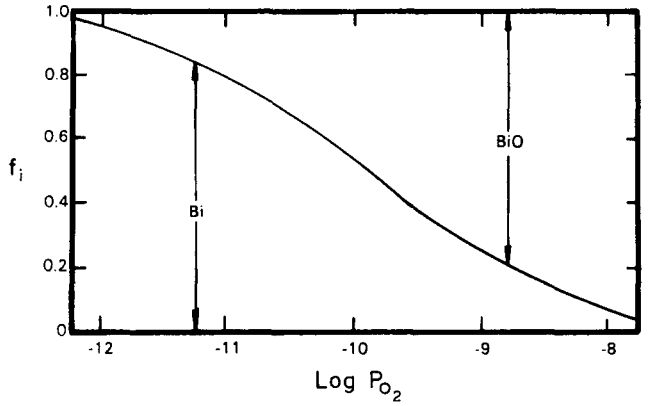


Fig. 11 — Fraction of the two forms of bismuth in slag at 1523 K and $P_{Bi}$ equal to $7.5 \cdot 10^{-4}$ atm.

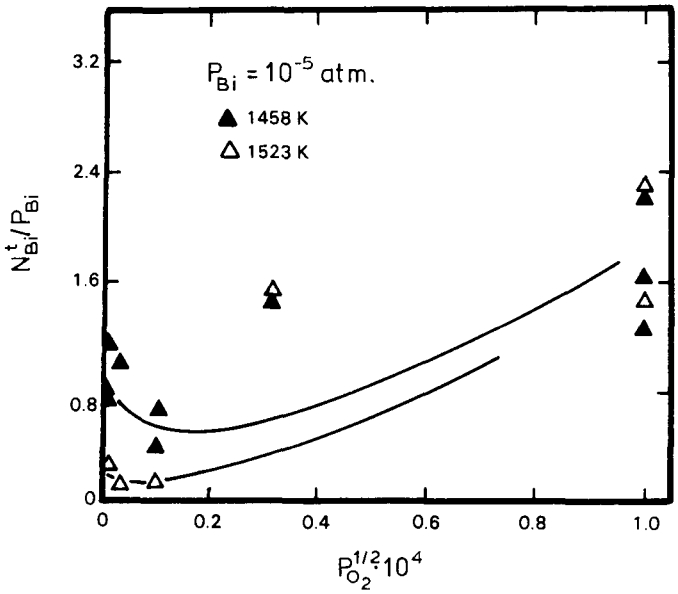


Fig. 12 — Solubility of bismuth in silica-saturated slags as represented by Eq. [15] ($P_{Bi} = 1 \cdot 10^{-5}$ atm).

influenced by slag composition. In both figures the solubility of bismuth in slag appears to decrease slightly as $P_{O_2}$ is increased from $10^{-12}$ to $10^{-10}$ atm. This is particularly apparent in the results shown in Figure 12 where the values of $N'/P_{Bi}$ are plotted *vs* $P^{1/2}_{O_2}$. No such minimum was observed with the data obtained at the higher value of $P_{Bi}$, as shown in Figure 9. A possible explanation for this behavior involves the structure of slag, and the influence slag composition may have on available sites for neutral bismuth.

**Table X. Comparison of Solubility of Neutral Bismuth**

| $P_{Bi}$ (atm) | $T$ (K) | $N^e \cdot 10^6$* |
|---|---|---|
| $10^{-5}$ | 1523 | 1.9 |
| $7.5 \cdot 10^{-4}$ | 1523 | 2.3 |
| $10^{-5}$ | 1458 | 7.0 |
| $7.5 \cdot 10^{-4}$ | 1458 | 19. |

*Calculated using Eq. [6] and activity coefficients in Table IX.

G. *Apparent Contradictions*

The results presented in Table IX, and in Figures 5 through 8, indicate that there are some apparent contradictions in the data. The most obvious seeming contradiction is found in the values of $\gamma_{Bi}$ in Table IX. The values for $\gamma_{Bi}$ that were obtained from the experiments conducted at the lower partial pressure of Bi ranged from 55 to 106 and are substantially smaller than the values obtained from the experiments conducted at the higher value of $P_{Bi}$. Those values should be similar, because activity coefficients are, in general, assumed to remain constant for dilute solutes in a relatively constant solvent.

The reduction in the activity coefficient suggests that elemental bismuth is more soluble in slag at lower partial pressures of Bi. That hypothesis is in conflict with Eq. [6] assuming a constant value for $\gamma_{Bi}$.

Bismuth is a large atom that, when present as a neutral atom in slag, must occupy a large hole in the structure. The number of those sites depends upon temperature, the angle between covalent bonds, and the coulombic interaction between ions.

As Bi vapor dissolves in slag the sites large enough to accommodate neutral bismuth become filled. When the number of vacant sites approaches zero, increasing the partial pressure of Bi will have little effect on the solubility of neutral bismuth. This phenomenon translates in quantitative terms into an increase in $\gamma_{Bi}$ with an increase in $P_{Bi}$.

As the values for the activity coefficient for neutral Bi are relatively large at $P_{Bi}$ equal to $10^{-5}$ atm (see Table IX), it can be assumed that most of the sites for neutral Bi are occupied and that any further increase in $P_{Bi}$ will not significantly increase the solubility of neutral Bi in slag. This hypothesis can be tested by calculating the solubility associated with neutral Bi at the higher partial pressure of Bi, and comparing the results with those obtained at the lower value of $P_{Bi}$. The results of that analysis are presented in Table X. Table X indicates that the mole fractions for neutral Bi in slag for the two values of $P_{Bi}$ are almost identical at 1523 K. The values are similar at 1458 K with $N^e$ higher at the higher value of $P_{Bi}$. The difference at 1498 K is most likely due to the scatter in the data at the higher partial pressure of Bi (see Figure 6). The scatter affects the regression analysis and thus the value of $\gamma_{Bi}$ and $N^e$.

Analysis of the results obtained in other studies further confirms the hypothesis that $\gamma_{Bi}$ is dependent upon the fraction of filled sites. Nagamori *et al.* reported that only neutral bismuth dissolved in slag.[1] They conducted those experiments at bismuth activities of $7.4 \cdot 10^{-4}$ to $1.9 \cdot 10^{-3}$. As shown in Table XI, those values compare favorably with the activities used in the present work at the lower partial pressure of bismuth. As noted above, the results obtained with the lower value of $P_{Bi}$ indicated neutral dissolution of Bi in slag.

Goto and coworkers reported only oxidic dissolution of bismuth in slag.[5] They conducted their experiments at a bismuth activity "on the order of $10^{-2}$." That activity, as shown in Table XI, is similar to that associated with the experiments conducted at the higher partial pressure of Bi in the present work. Those experiments, like the work of Goto *et al.*, yielded a strong indication of oxidic dissolution.

See and Rankin,[2] using a procedure similar to Nagamori *et al.*,[1] concluded that bismuth exists as a neutral species in

**Table XI. Comparison of Results and Activity of Bi Used in Several Studies**

| Investigators | $a_{Bi}$ | Results |
|---|---|---|
| Present work | $2.4 \cdot 10^{-4}$ to $4.8 \cdot 10^{-4}$ | primarily neutral dissolution |
| Present work | $1.8 \cdot 10^{-2}$ to $3.6 \cdot 10^{-2}$ | oxidic dissolution |
| Nagamori, Mackey, and Tarassoff[1] | $7.4 \cdot 10^{-4}$ to $1.9 \cdot 10^{-3}$ | neutral dissolution |
| Jimbo, Goto, and Ogawa[5] | approximately $10^{-2}$ | oxidic dissolution |
| See and Rankin[2] | $10^{-3}$ to $10^{-2}$ | reported neutral dissolution but conducted experiments at the higher activity of Bi at only one value of $P_{O_2}$ |

slag. They conducted their experiments at bismuth activities of approximately $10^{-2}$ and $10^{-3}$. Unfortunately, the equilibrations at the latter activity were conducted over the range of $P_{O_2}$ values from $10^{-9}$ to $10^{-7}$ atm. Those data, coupled with the experimental results obtained at the higher activity for bismuth and $P_{O_2}$ equal to $5 \cdot 10^{-8}$ atm, mask any influence $P_{O_2}$ has on the solubility of bismuth in slag. Furthermore, those researchers expressed concern that the distribution of bismuth between slag and metal may not have been at equilibrium.

## VI. CONCLUSIONS

Bismuth has been shown to enter slag in two forms, elemental and oxidic. The data indicate that the latter form of bismuth in slag is BiO. The experimental results obtained in this study indicates that $\gamma_{Bi}$ varies significantly with the solubility of neutral bismuth in slag. It has been hypothesized, based on the large diameter of neutral Bi, that there are a limited number of sites that can accommodate neutral Bi, and that as that limit is approached $\gamma_{Bi}$ increases significantly. That hypothesis has been shown to be consistent with the experimental results obtained in the present work as well as the results obtained by other investigators.

## APPENDIX A

### Evaluation of thermal mass diffusion equations

The concentration and thermal diffusion fluxes in the derivation of Eq. [2] are presented below. The derivation is extracted from Bird, Stewart, and Lightfoot,[37] and Grew and Ibbs.[38] The concentration flux ($j_i^X$) and thermal diffusion flux ($j_i^T$) are:

$$j_i^X = \frac{c^2}{\rho R T} \sum_{j=1}^{n} M_i M_j D_{ij} \left[ X_j \sum_{\substack{k=1 \\ k \neq j}}^{n} \left( \frac{\partial \overline{G}_j}{\partial X_k} \right)_{T,P,X_s \atop s \neq j,k} \nabla X \right] \quad [A1]$$

$$j_i^T = -D_i^T \nabla \ln T \quad [A2]$$

where $c$ = molar concentration ($M/L^3$).
$\rho$ = mass concentration ($M/L^3$).
R = gas constant.
$T$ = temperature.
$M_i, M_j$ = molecular weight of species $i$ and $j$.
$D_{ij}$ = multicomponent diffusivity of the $i$-$j$ pair in a multicomponent gas mixture ($L^2/t$).
$X_j$ = mole fraction of species $j$.
$G_j$ = partial molar Gibbs energy of species $j$ in the multicomponent gas mixture.
$D_i^T$ = multicomponent thermal diffusion coefficient for component $i$ in a multicomponent gas mixture (M/Lt).
$\nabla$ = vector differential operator with respect to rectangular coordinates.

It should be noted that $D_{ij}$ and $D_i^T$ have the following properties:

$$D_{ii} \neq 0 \quad [A3]$$

$$\sum_{i=1}^{n} D_i^T = 0 \quad [A4]$$

$$\sum_{i=1}^{n} (M_i M_h D_{ih} - M_i M_k D_{ik}) = 0 \quad [A5]$$

However, for cases where $n > 2$ (a nonbinary system), $D_{ij}$ and $D_{ji}$ are not usually equal.

Continuing the development for a binary system represented by $A$ and $B$, the sum of Eqs. [A1] and [A2] becomes:

$$j_A = \frac{c^2}{\rho R T} \left\{ M_A M_A D_{AA} \left[ X_A \left( \frac{\partial \overline{G}_A}{\partial X_A} \right)_{T,P} \nabla X_A \right] + M_A M_B D_{AB} \left[ X_B \left( \frac{\partial \overline{G}_B}{\partial X_A} \right)_{T,P} \nabla X_A \right] \right\} - D_A^T \nabla \ln T \quad [A6]$$

Since $D_{AA} = 0$,

$$j_A = \frac{c^2}{\rho R T} M_A M_B D_{AB} \left[ X_B \left( \frac{\partial \overline{G}_B}{\partial X_A} \right)_{T,P} \nabla X_A \right] - D_A^T \nabla \ln T \quad [A7]$$

Now, for an ideal binary gas mixture, the Gibbs-Duhem equation is:

$$X_A \left( \frac{\partial \overline{G}_A}{\partial X_A} \right)_{T,P} + X_B \left( \frac{\partial \overline{G}_B}{\partial X_A} \right)_{T,P} = 0 \quad [A8]$$

and

$$X_A \left( \frac{\partial \overline{G}_A}{\partial X_A} \right)_{T,P} = -X_B \left( \frac{\partial \overline{G}_B}{\partial X_A} \right) \quad [A9]$$

Substitution of Eq. [A9] into Eq. [A7] yields:

$$j_A = \frac{c^2}{\rho R T} M_A M_B D_{AB} \left[ -X_A \left( \frac{\partial \overline{G}_A}{\partial X_A} \right)_{T,P} \nabla X_A \right] - D_A^T \nabla \ln T \quad [A10]$$

Also, by assuming an ideal gas mixture:

$$d\overline{G}_A = RT d \ln a_A = RT d \ln X_A \quad [A11]$$

And by introducing a thermal diffusion ratio,

$$k_T = \frac{D_A^T}{c^2 M_A M_B D_{AB}} \quad [A12]$$

Eq. [A10] may be reduced to:

$$j_A = \frac{-c^2}{\rho} M_A M_B D_{AB} \left( \frac{dX_A}{dZ} + \frac{k_T}{T} \frac{dT}{dZ} \right). \quad [A13]$$

The establishment of steady state results in a condition of no net mass flux, resulting in $j_A = 0$, and:

$$0 = \frac{-c^2}{\rho} M_A M_B D_{AB} \left( \frac{dX_A}{dZ} + \frac{k_T}{T} \frac{dT}{dZ} \right). \quad [A14]$$

Following the procedure as reported by Bird, Stewart, and Lightfoot,[37] the solution to this differential equation yields:

$$X_{A_2} - X_{A_1} = -k_T \ln \frac{T_2}{T_1} \quad [A15]$$

This equation shows that the change in composition of $A$ depends on the difference in temperature between each end of the experimental tube through $k_T$. The thermal diffusion ratio, $k_T$, depends on the following factors:

(a) The ratio of the two species' masses and of their diameters.
(b) The nature of the intermolecular forces between the two molecules and also between like molecules.
(c) The proportions ($X_A, X_B$) of the two components. Since $k_T$ contains terms involving the molar densities and molecular weights, $k_T$ depends on the mole fraction of each component.

Since $k_T$ depends on intermolecular interactions and molecular concentration, then $k_T$ may be described through a series of collision integrals. Grew and Ibbs[38] have shown that through this method the thermal diffusion ratio may be approximated by the relationship:

$$k_T = 5(Z - 1) \frac{S_A X_A - S_B X_B}{Q_A X_A^2 + Q_B X_B^2 + Q_{AB} X_A X_B} \cdot X_A X_B \quad [A16]$$

The functions $S$ and $Q$ depend on the collision integrals and mass ratios, and for monatomic and diatomic bismuth vapor species

$$S_{Bi} = -0.643 \quad [A17]$$

$$S_{Bi_2} = 0.515 \quad [A18]$$

$$Q_{Bi} = 4.177 \quad [A19]$$

$$Q_{Bi_2} = 2.886 \quad [A20]$$

$$Q_{Bi-Bi_2} = 9.183 \quad [A21]$$

$$Z = 6/5 \quad [A22]$$

Analysis of those constants required evaluation of the molecular diameters Bi and $Bi_2$. In the Bi, $Bi_2$ gas mixture, the molecular diameter of Bi is 3.20 Å while that of $Bi_2$ is approximately 4.58 Å. The value for $Bi_2$ was found by the following method.

The $Bi_2$ gas molecule is not found as a sphere, but as a molecule of a cylindrical shape. By using the covalent radius and the Born-Slater radius for Bi, the size of the cylinder can be estimated. Figure A1 illustrates the concept of the two Bi atoms forming the $Bi_2$ molecule. Due to the overlapping of the bonding orbitals, the distance between the two nuclei is more accurately estimated by using the covalent bond radius. The Born-Slater radius may be used to compute the length of the molecule as well as the width of the molecule since the Bi orbitals will be less perturbed in those directions. The bond angle between the atoms is ignored for these calculations.

The volume of this cylinder is calculated, then the radius of a hypothetical $Bi_2$ spherical molecule is found from this volume.

$$\pi r_{B-S}^2 L = 50.19 \text{ Å}^3 \quad [A23]$$

$$50.19 \text{ Å}^3 = \frac{4}{3} \pi (r_{Bi_2}^*)^3 \quad [A24]$$

$$r_{Bi_2}^* = 2.29 \text{ Å} \quad [A25]$$

The superscript * represents that this value is a hypothetical radius for a $Bi_2$ spherical molecule. This value is only 0.69 Å larger than the radius of Bi gas, and is most likely small. The bond angle between Bi atoms was ignored for this reason. As a first approximation this is a good estimate.

The value of $k_T$ may be found when the mole fractions of Bi and $Bi_2$ in the gas phase are known. Brown[39] (from Grew and Ibbs[38]) has shown that when the separation of the gas phase is small, but measurable, only an average value of $k_T$ can be found. This value will be found at a mean temperature:

$$T_m = \frac{T_1 T_2}{T_2 - T_1} \ln \frac{T_2}{T_1} \quad [A26]$$

Since the value of $k_T$ will be known only at $T_m$, then the bismuth gas phase composition must also be known at this temperature. The gas phase composition was found by using existing thermodynamic data for Bi vapor species in an iterative computer code that utilized the values of $T_m$ in the calculations. The results are shown in Table AI. From these values, four values of $k_T$ may be found, each representing a particular set of conditions used in this study. The values of $k_T$ are shown in Table V, along with the corresponding separation expressions, $X_{A2} - X_{A1}$.

## APPENDIX B

### Iron analysis

Since the isopiestic experimental system is a closed system, the oxygen partial pressure over a slag is not directly measurable. The partial pressure of oxygen, however, is a function of the ferrous/ferric ion ratio.

The method developed to evaluate the ferrous/ferric ion ratio is a modification of one first proposed by Harvey, Smart, and Amis.[33] The method utilizes the principle of complexing iron with an organic reagent, 1,10-phenanthroline, to form colored complexes that can be used to determine the iron content of a sample. An oxygen-free environment is essential in preventing oxidation of iron (II) during digestion and analysis. The system shown schematically in Figure B1 meets the inert atmosphere requirements. The analytical procedure is discussed below.

Slag samples weighing between 0.028 and 0.035 grams were placed in 100 ml Pyrex vials. The slags were wetted

with 3 ml 6M HCl and then the vials were capped. The caps were designed to allow continuous purging of the vials by $N_2$. A schematic representation of the digestion vials is shown in Figure B2. After a 24-hour digestion period, the vials were opened and poured into the iron analysis apparatus, which was continually purged with nitrogen gas (see Figure B1). The solution was diluted to 1000 ml with distilled water in a round bottom flask during the first step of the procedure. This solution was then divided into two 500 ml portions by pumping the solution into two calibrated 500 ml round bottom flasks. These solutions were then pumped into two 2000 ml volumetric flasks. One flask contained 100 ml saturated 1,10-phenanthroline solution, and the other flask contained 200 ml of 2 wt pct hydroquinone solution. This procedure gave an effective dilution volume of 4000 ml. A period of one-half hour was allowed for the hydroquinone to reduce all the iron in the second flask to iron (II). The iron in this flask was complexed by syringe injection of 100 ml of saturated 1,10-phenanthroline solution. The solutions were then brought to final volume by adding distilled water.

Finally, the solutions were analyzed on a Bausch and Lomb Spectronic 21 optical spectrophotometer for absorbance at 512 nm. The contents of the first flask yield iron (II); the second flask gives the total iron absorbance. Concentrations are determined by comparison to known standard iron solutions. The standards and blanks were matrix matched to the two iron solutions. This was accomplished by adding the appropriate amount of 2 wt pct hydroquinone and 1,10-phenanthroline solution to the blanks. This effectively eliminated the minor absorption of both hydroquinone and 1,10-phenanthroline at 512 nm. Iron (III) was found by subtracting iron (II) (first flask) from the total iron (second flask). Undigested silica did not present a problem during the analyses, as the undigested silica particles settled out of solution.

A sample of Minorca ore supplied by the USBM containing 22.2 wt pct $Fe^{2+}$ and a total iron content of 69.1 wt pct was used to evaluate the analytical procedure. Evaluation of analyses of 4.0 ppm $Fe^{2+}$ solutions prepared from the ore yielded a standard deviation of 0.22 ppm. Linear absorbance at 512 nm was found to occur up to 5 ppm $Fe^{2+}$.

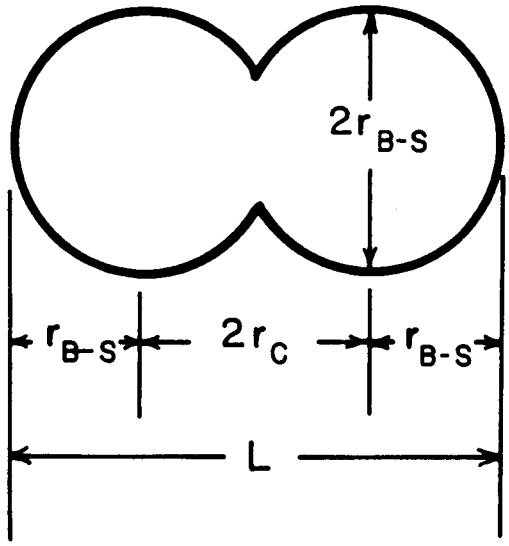


Fig. A1 — Conceptual representation of the $Bi_2$ molecule. The Born-Slater radius is represented by B-S, while the covalent radius is represented by C. $r_C$ = 1.52 Å, $r_{B-S}$ = 1.60 Å.

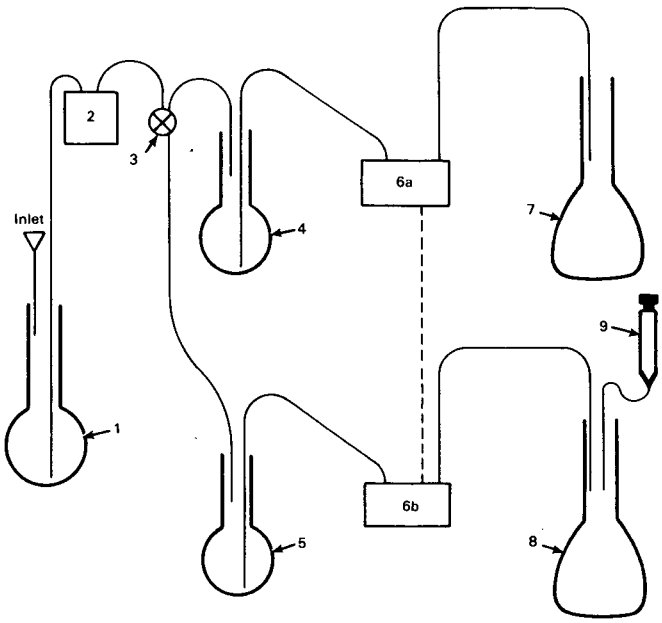


Fig. B1 — Schematic of iron analysis equipment: (1) calibrated 1000 ml round bottom flask, (2) peristaltic pump, (3) glass valve, (4) calibrated 500 ml round bottom flask, (5) calibrated 500 ml round bottom flask, (6) peristaltic pump (2nd pump heads), (7) 1000 ml volumetric flask, (8) 1000 ml volumetric flask, and (9) 50 ml syringe. Note: $N_2$ inlets, outlets, and stoppers for the flasks are not illustrated.

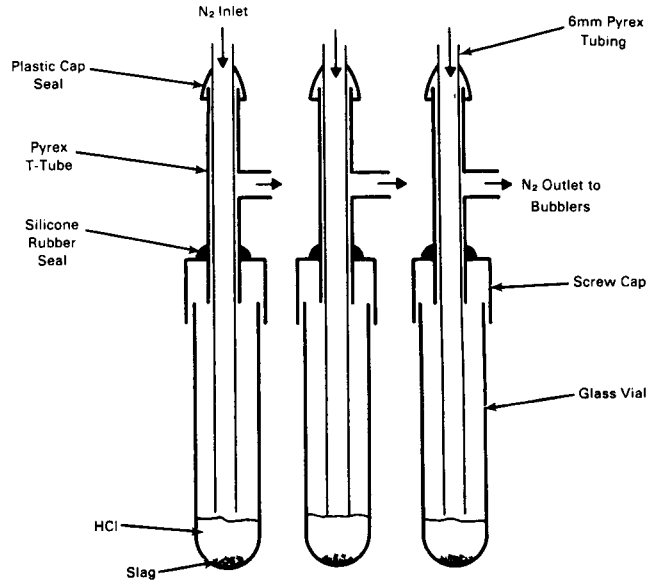


Fig. B2 — Slag digestion vials with inert atmosphere capability.

## ACKNOWLEDGMENT

Financial support for this investigation was provided by the United States Bureau of Mines (Contract No. J0215019). Their support is gratefully acknowledged.

**Table AI. Gas Phase Composition within the Isopiestic System**

| Slag Temp. (K) | Source Temp. (K) | Mean Temp. (K) | $P_{Bi}$ (atm) | $P_{Bi_2}$ (atm) | $X_{Bi}$ | $X_{Bi_2}$ |
|---|---|---|---|---|---|---|
| 1458 | 942 | 1162 | $8.5 \cdot 10^{-6}$ | $2.1 \cdot 10^{-6}$ | 0.800 | 0.200 |
| 1523 | 942 | 1186 | $1.0 \cdot 10^{-5}$ | $1.6 \cdot 10^{-7}$ | 0.985 | 0.015 |
| 1458 | 1131 | 1281 | $4.9 \cdot 10^{-4}$ | $7.9 \cdot 10^{-5}$ | 0.860 | 0.140 |
| 1523 | 1131 | 1308 | $5.1 \cdot 10^{-4}$ | $5.8 \cdot 10^{-5}$ | 0.898 | 0.102 |

## REFERENCES


1. M. Nagamori, P. J. Mackey, and P. Tarassoff: *Metall. Trans. B*, 1975, vol. 6B, pp. 295-301.
2. J. B. See and W. J. Rankin: National Institute for Metallurgy, Report 2099, 1981.
3. E. A. Johnson, P. E. Sanker, L. L. Oden, and J. B. See: United States Bureau of Mines, RI 8655, 1982, 18 pp.
4. S. Goto, O. Ogawa, and I. Jimbo: *Australia-Japan Extractive Metallurgy Symp. Proc.*, Australian Institute of Metallurgy, Sydney, Australia, 1980, pp. 127-32.
5. I. Jimbo, S. Goto, and O. Ogawa: *Metall. Trans. B*, 1984, vol. 15B, pp. 535-41.
6. A. Roine: *Metall. Trans. B*, 1987, vol. 18B, pp. 203-12.
7. A. Roine and H. Jalkanen: *Metall. Trans. B*, 1985, vol. 16B, pp. 129-41.
8. N. Asano and M. Wada: *Suiyokaishi*, 1968, vol. 16, pp. 385-88.
9. S. Arac and G. H. Geiger: *Metall. Trans. B*, 1981, vol. 12B, pp. 569-71.
10. T. Azakami and A. Yazawa: *Can. Metall. Q.*, 1976, vol. 15, pp. 111-22.
11. V. S. Sibanda and E. H. Baker: *IMM Trans. C.*, 1979, vol. 88, pp. C129-30.
12. V. J. Bode, J. Gerlach, and F. Pawlek: *Erzmetal.*, 1971, vol. 24, pp. 480-85.
13. G. K. Sigworth and J. F. Elliott: *Can. Metall. Q.*, 1974, vol. 13, pp. 455-61.
14. B. Predell and A. Emam: *Zhurnal Metallk.*, 1973, vol. 64, pp. 496-501.
15. D. L. Hildebrand and K. H. Lau: Progress Report, Sept. 1979 to June 1980, NSF Grant DAR 79-12296, SRI Project Number 8933.
16. S. Arac: Ph.D. Thesis, University of Arizona, Tucson, AZ, 1980.
17. P. Taskinen: *Scand. J. of Metal.*, 1982, vol. 11, pp. 150-54.
18. P. Taskinen and J. Niemela: *Scand. J. of Metal.*, 1981, vol. 10, pp. 195-200.
19. D. C. Lynch and K. W. Schwartze: *Can. Metall. Q.*, 1981, vol. 20, pp. 269-78.
20. R. F. Farrell, S. A. Matthes, and A. J. Mackie: United States Department of the Interior, Bureau of Mines, RI 8480, 1980, 14 pp.
21. L. N. Sidorov, I. I. Minayeva, E. Z. Zasorin, I. D. Sorokin, and A. Y. Borschchevskiy: *High Temp. Sci.*, 1980, vol. 12, pp. 175-96.
22. V. S. Ban and B. E. Knox: *Chem. Phys.*, 1970, vol. 52, pp. 243-47.
23. V. K. Il'in: *Zhur. Neorg. Khim.*, 1976, vol. 21, pp. 1645-48.
24. C. K. Kazenas, D. M. Chizhikov, Y. U. Tsvetkov, and M. V. Ol'shevskii: *Doklady Akad. Nauk. SSSR*, 1972, vol. 207, pp. 354-55.
25. O. M. Uy and J. Drowart: *Trans. Faraday Soc.*, 1969, vol. 65, pp. 3221-30.
26. L. B. Pankratz: "Thermodynamic Properties of Elements and Oxides," U.S. Bureau of Mines Bulletin 672, 1982.
27. F. J. Kohl, O. M. Uy, and K. D. Carlson: *J. Chem. Phys.*, 1967, vol. 47, pp. 2607-76.
28. L. Rovner, A. Drowart, and J. Drowart: *Trans. Faraday Soc.*, 1967, vol. 63, pp. 2906-11.
29. C. L. Sullivan, J. K. Prusaczyk, and K. D. Carlson: *High Temp. Sci.*, 1972, vol. 4, pp. 212-22.
30. L. C. Wagner and R. T. Grimely: *Chem. Phys. Letters*, 1974, vol. 29, pp. 594-99.
31. G. H. Geiger and D. R. Poirier: *Transport Phenomena in Metallurgy*, Addison-Wesley, Reading, MA, 1973, p. 470.
32. G. D. Christian: *Analytical Chemistry*, 2nd ed., John Wiley & Sons, New York, NY, 1977, pp. 320-25.
33. A. E. Harvey, J. A. Smart, and E. S. Amis: *Anal. Chem.*, 1955, vol. 27, pp. 26-29.
34. M. Nagamori and P. J. Mackey: *Metall. Trans. B*, 1977, vol. 8B, pp. 39-46.
35. L. Fang and D. C. Lynch: *Metall. Trans. B*, 1987, vol. 18B, pp. 181-87.
36. O. Kubaschewski and C. B. Alcock: *Metallurgical Thermo-Chemistry*, 5th ed., Pergamon, Oxford, England, 1979, pp. 179-207.
37. R. B. Bird, W. E. Stewart, and E. N. Lightfoot: *Transport Phenomena*, John Wiley and Sons, New York, NY, 1960, pp. 567-72.
38. K. E. Grew and T. L. Ibbs: *Thermal Diffusion in Gases*, New York: Cambridge University Press, 1952.
39. H. Brown: *Phys. Rev.*, 1940, vol. 58, pp. 661-62.